Rotational Spectroscopy

DOI: 10.1002/anie.201403838

Chirality Induction and Amplification in the 2,2,2-Trifluoroethanol···Propylene Oxide Adduct**

*Javix Thomas, Wolfgang Jäger, and Yunjie Xu**

Abstract: *Chirality induction and amplification in a model system, that is, the 2,2,2-trifluoroethanol (TFE)···propylene oxide (PO) adduct, were investigated using free-space and cavity-based Fourier transform microwave spectroscopy, complemented with high level ab initio calculations. Rotational spectra of four out of eight predicted TFE··PO adducts were assigned, and the remaining four were shown to relax to the geometries of the four observed in a jet expansion. The g+ TFE···S-PO adduct was found to be favored over that of g− TFE···S-PO by a factor of 2.8 at 60 K. This difference contrasts the TFE dimer for which an extreme case of chirality synchronization was previously reported. All TFE···PO conformers observed take on the open arrangement, in contrast to 2-fluoroethanol···PO, which prefers the closed arrangement. Furthermore, perfluorination at CH_3 increases the hydrogen-bonding energy by about 70% over its ethanol counterpart.*

Chirality induction, a special form of chirality recognition,[1] is at the heart of stereoselective syntheses, such as chiral hydrogenations,[2] chiral bio-organic synthesis,[3] synthesis of inorganic and inorganic-organic chiral porous solids,[4] and the design of chiral polymers.[5] Starting from permanently chiral chemical reactants and/or catalysts, new chirality is induced in the activated complex or reaction intermediate which consist of the chiral species and prochiral or transiently chiral molecules. This process eventually results in one or more new permanent stereogenic centers, or helicity of the product, often with significant preference for one specific handedness, and is termed chirality amplification.[5] Some solvents, such as 2,2,2-trifluoroethanol (TFE), are known to promote such chirality induction and amplification processes.[6–8] For example, TFE is widely used as a peptide cosolvent for structural function investigations of protein and peptide folding processes in aqueous solution. The intermolecular interactions of TFE with peptides and proteins can alter their secondary and tertiary structures, thereby facilitating the protein folding process.[7,9–11] In a recent solid-state NMR study, its derivative, phenyl TFE, was used as a chiral solvating agent for enantioselective separation for a number of chiral metal–organic frameworks.[12] Hydrogen bonding and other non-covalent interactions between chiral units and TFE are rationalized to be responsible for the observed chirality induction.[13,14]

Jet-cooled rotational spectroscopy is well known for providing accurate structural and relative stability information for benchmarking theoretical modeling of important intermolecular interactions.[15–19] Because of its high-resolution nature, it can distinguish between conformers with only minute structural differences, free of perturbations by the environment, and allows unambiguous identification of individual conformers independently of theoretical modeling. With the advent of broadband chirped pulse Fourier transform microwave (CP-FTMW) spectroscopy,[20] major progress has been made in rotational spectroscopic studies of systems with a large number of conformers.[15,16] Broadband rotational spectroscopy offers the great advantage of being able to detect all relevant conformers simultaneously and does not require a microwave resonator. The latter helps to overcome the well-known challenges associated with resonator-based FTMW experiments, such as intensity variations for different transitions resulting from resonator-mode adjustments and sample fluctuations.

Herein we report free-space and cavity-based rotational spectroscopic and ab initio studies of the TFE···PO (PO = propylene oxide) adduct. TFE can adopt three conformations: *gauche* + (*g* +), *gauche*− (*g*−), and *trans* (*t*), but only the *gauche* forms were observed in gas-phase spectroscopic studies.[21,22] In those studies, evidence for a tunneling motion between the two isoenergetic *gauche* forms was found.[21,22] Of particular interest are the FTIR studies of the TFE dimer in which an extreme case of chirality synchronization, facilitated by an incoherent tunneling motion, was reported: only the homochiral dimer was detected and no evidence for the energetically competitive heterochiral dimer was found in the experiment.[1,14] Equipped with the advantages of broadband CP-FTMW spectroscopy and the ultrahigh resolution of cavity-based FTMW measurements, we aimed to find definite answers for some interesting questions: What hydrogen-bonding topologies will the TFE···PO conformers take on? Will chirality induction in TFE···PO favor the *g* + or *g*− TFE form exclusively? This scenario would be similar to the TFE dimer case where one monomer appears to almost quantitatively assume the handedness of the other.[14]

We explored the conformational landscape of the TFE···PO adduct with ab initio calculations at the MP2/6-311 + + G(2d,p) level of theory using the Gaussian 09 suite of programs.[23] Eight binary conformers (Figure 1) were identi-

[*] J. Thomas, Prof. Dr. W. Jäger, Prof. Dr. Y. Xu
Department of Chemistry, University of Alberta
Edmonton, AB, T6G 2G2 (Canada)
E-mail: yunjie.xu@ualberta.ca

[**] This research was funded by the University of Alberta and the Natural Sciences and Engineering Research Council (NSERC) of Canada. We also gratefully acknowledge access to the computing facilities of the Shared Hierarchical Academic Research Computing Network (SHARCNET: www.sharcnet.ca), the Western Canada Research Grid (Westgrid), and Compute/Calcul Canada. W.J. and Y.X. are holders of Tier I Canada Research Chairs.

Supporting information for this article is available on the WWW under http://dx.doi.org/10.1002/anie.201403838.

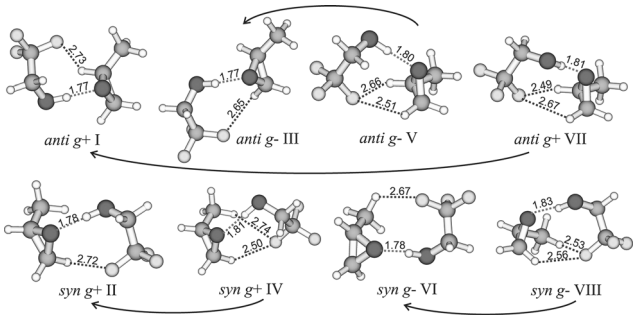

Figure 1. Structures of the eight most stable conformers of the TFE···PO adduct. The *syn* and *anti* designations refer to whether TFE approaches PO from the same or opposite sides of the PO methyl group, respectively. Roman numerals I to VIII label the relative stability starting from the most stable one. The numbers represent intermolecular bond lengths in Å. The arrows indicate the conformational relaxation under jet expansion conditions. See the text for discussions.

fied and confirmed to be true minima without imaginary frequencies. While the abundance ratio of the *trans* to the *gauche* configurations in liquid TFE was reported to be 40:60,[24] all binary structures starting with *t* TFE converged to either *g*+ or *g*− TFE···PO conformers, thus strongly suggesting that *t* TFE is still unstable in the hydrogen-bonded binary adduct.[14,21] The calculated dissociation energies, rotational constants, and electric dipole moment components of all eight binary adducts are summarized in Table 1. Since the energy differences among the eight conformers are generally small, one may be able to see all of them in a jet. In contrast, given that the TFE subunit in TFE···PO experiences similar hydrogen-bonding interactions as in the TFE dimer, one wonders if the permanent chirality of PO will induce a strong chiral preference in the TFE subunit. This preference could be facilitated by a fast interconversion between *g*+ and *g*− TFE, similar to the case of the TFE dimer.[14]

Table 1: Calculated relative raw dissociation energies ΔD_e, and the ZPE- and BSSE-corrected dissociation energies ΔD_0 (in kJ mol^{-1}), rotational constants *A*, *B*, and *C* (in MHz), and electric dipole moment components $|\mu_{a,b,c}|$ (in Debye) of the TFE···PO conformers.

Para.	I	II	III	IV	V	VI	VII	VIII
ΔD_e[a]	0	−0.85	−1.45	−1.25	−1.56	−0.83	−1.82	−3.05
ΔD_0[b]	0	−0.29	−0.49	−0.69	−0.91	−0.94	−1.12	−3.76
A	2161	2471	2954	2180	2360	2326	2306	2078
B	684	609	530	646	593	659	599	666
C	594	570	505	640	572	615	560	617
$\lvert\mu_a\rvert$	2.76	2.98	2.91	2.62	2.38	3.19	2.98	3.44
$\lvert\mu_b\rvert$	0.03	0.39	0.10	1.41	1.63	0.2	1.78	2.38
$\lvert\mu_c\rvert$	0.01	0.09	0.09	0.38	1.12	0.06	0.57	0.52

[a] $\Delta D_e(i) = D_e(i) - D_e(I)$ where i = I to VIII and $D_e(I) = 41.92$ kJ mol^{-1}.
[b] $\Delta D_0(i) = D_0(i) - D_0(I)$ where i = I to VIII and $D_0(I) = 27.70$ kJ mol^{-1}.

Broadband spectra of samples containing TFE or PO or both together in helium (or neon) were recorded separately in the frequency range from 7.7 to 10.5 GHz using a CP-FTMW spectrometer.[25] Very dense spectra were obtained. To aid the spectral assignments of TFE···PO, transitions resulting from $(PO)_n$, $(TFE)_n$, $(PO)_n(RG)_m$, or $(TFE)_n(RG)_m$ (with RG = He or Ne; n, $m = 1, 2, \ldots$) were first removed. Four sets of rotational transitions resulting from TFE···PO were assigned, and the experimental and assignment details are provided in the Supporting Information. The final transition frequencies were measured using a resonator-based[26] coaxial pulsed jet FTMW spectrometer[27] and were fitted using Watson's S-reduction Hamiltonian in the I^r representation[28] with the Pgopher program.[29] The standard deviations for all fits are less than 2.5 kHz, similar to the uncertainty of the experimental measurements. Transition frequencies and the corresponding quantum number assignments of all the observed transitions are given in Tables S1–S5 in the Supporting Information. The experimental spectroscopic constants obtained are listed in Table 2.

Table 2: Experimental spectroscopic constants of the four TFE···PO conformers.

P[a]	I	II	III	VI
A	2170.106(11)	2426.6781(19)	2920.124(71)	2336.440(30)
B	652.14861(29)	594.67934(12)	516.98121(23)	632.57360(30)
C	569.66525(28)	560.17041(12)	491.67870(22)	589.52799(23)
D_J	0.42182(64)	0.26478(28)	0.16888(37)	0.42845(70)
D_{JK}	0.4354(25)	0.7830(15)	0.2175(40)	−0.8296(37)
D_K[b]	0.00	5.80(40)	0.00	0.00
d_1	−0.0713(11)	−0.00249(40)	−0.00129(60)	0.02034(85)
d_2[b]	0.00	−0.00232(16)	0.00	0.0
N	50	52	43	45
Σ	2.2	1.2	1.9	2.4

[a] Rotational constants in MHz and distortion constants in kHz. *N* is the number of transitions included in the fit and σ (in kHz) is the standard deviation of the fit. Standard errors within parentheses are expressed in units of the last digit. [b] D_K and d_1 were kept at 0.0 in the fit because only *a*-type transitions were observed for conformers I, III, and VI.

By comparison of the experimental and theoretical rotational constants and especially the relative intensities of the *a*-, *b*-, and *c*-type transitions, the four observed conformers were clearly identified as I, II, III, and VI. A maximum deviation of 4.6 % was observed between the experimental and theoretical rotational constants for a particular assigned conformer, still allowing unambiguous correlation of the observed conformers with the calculated ones. No additional splitting was detected for any of the observed TFE···PO transitions, despite the high resolution capability of the cavity spectrometer. This observation is expected since the *g*+ and *g*− TFE subunits are locked into their respective configurations in the binary adducts, along with large structural and thus also energetic differences.

The *a*-type electric dipole moment components are predicted to be similar for all four observed conformers. Using the calculated *a*-dipole moment components, the relative abundances of the conformers were estimated to be: I/II/III/VI = 1:0.75:0.35:0.40 based on the intensities of the *a*-type transitions in the broadband spectra (see the Supporting Information for details). Among the assigned binary conformers, I and II, formed by *S*-PO and *g*+ TFE, are favored over III and VI, which consist of *S*-PO and *g*− TFE. In addition, no transitions resulting from the conformers IV

and V were observed in the broadband spectrum even though they are predicted to be more stable than the assigned conformer VI.

To address the above observations, we examined the subtle balance between the inter- and intramolecular hydrogen bonds in the binary adducts, the factors that contribute to the stability, and possible conformational relaxation in the jet expansion. The dissociation energy, D_e, can be decomposed into $E^{dist}_{PO} + E^{dist}_{TFE} + E^{int}$, as defined in reference [30]. Here, E^{dist}_{PO} and E^{dist}_{TFE} are the monomer deformation energies for PO and TFE, respectively, and correspond to the energy penalty for distorting the isolated monomers from their equilibrium geometries to the ones in the TFE···PO complex. E^{int} is the interaction energy of the binary complex and is the difference between the total dimer energy and the energy of the two monomeric PO and TFE units in the TFE···PO dimer. The values of these terms are summarized in Table 3, together with the values of the basis set superposition error (BSSE) and zero-point energy (ZPE) corrections.

Table 3: The calculated deformation, interaction, raw dissociation energies, and BSSE and ZPE corrections (in kJ mol^{-1}) at the MP2/6-311++G(2d,p) level for the eight predicted conformers of TFE···PO.

Conformer	E^{dist}_{PO}	E^{dist}_{TFE}	E^{int}	D_e	BSSE	ZPE
I	−0.42	−1.28	43.62	41.92	−9.56	−4.66
II	−0.43	−1.38	42.87	41.07	−8.94	−4.72
III	−0.43	−1.34	42.24	40.46	−8.65	−4.61
IV	−0.43	−1.66	42.76	40.66	−9.08	−4.58
V	−0.38	−1.60	42.34	40.36	−8.97	−4.60
VI	−0.47	−1.00	42.56	41.09	−9.55	−4.79
VII	−0.36	−1.74	42.20	40.09	−8.99	−4.53
VIII	−0.32	−1.82	40.07	37.93	−8.85	−4.44
ΔE*(all conf.)*[a]	0.15	0.82	3.55	3.99	0.91	0.35
ΔE*(obs.conf.)*[a]	0.05	0.38	1.38	1.46	0.91	0.18

[a] Absolute maximum difference (in kJ mol^{-1}) among the eight predicted and four observed conformers, respectively.

From Table 3, it is clear that the deformation energies of PO are small and contribute little (≤ 0.15 kJ mol^{-1}) to the conformational preference. This small contribution is reasonable since PO is a fairly rigid molecule. The corresponding TFE deformation energies contribute modestly (≤ 0.82 kJ mol^{-1}), as do the BSSE corrections (≤ 0.91 kJ mol^{-1}). In comparison, the interaction energies are on the order of 42 kJ mol^{-1} and contribute decisively (≤ 3.55 kJ mol^{-1}) to the conformational preference among the eight conformers. It is also interesting to note that the ZPE corrections make only minor contributions to the relative conformational stability. Concerning the four conformers observed, both the interaction energies and the BSSE corrections are the dominant factors in determining the conformational preference.

A detailed comparison of the conformer geometries reveals that one can separate these structures into four groups: *anti* $g+$, *syn* $g+$, *anti* $g-$, and *syn* $g-$. One may expect that intergroup relaxation is not allowed in a jet expansion. For example, it is difficult for TFE to move from an *anti* position to a *syn* position in a jet expansion. The situation within each group is, however, different. Each group contains two structures, one is open with one F···H–C secondary hydrogen bond, while the other is closed with two F···H–C secondary hydrogen bonds. It can be hypothesized that the interconversion barrier between these two conformers in each group is low since it involves only small changes, such as breaking one weak F··H–C bond in favor of optimizing the existing primary intermolecular hydrogen bond and the other F··H–C bond. Indeed, the four experimentally detected conformers, that is, *anti* $g+$ I, *syn* $g+$ II, *anti* $g-$ III, and *syn* $g-$ VI, correspond to the open structure in each group, and are the more stable ones predicted in each group. The proposed conformational relaxations are indicated with arrows in Figure 1: IV→II, V→III, VII→I and VIII→VI. This hypothesis explains why IV and V could not be observed even though they were predicted to be more stable than VI.

The predicted Boltzmann ratio for I/II/III/VI is 1:0.73:0.48:0.14, taking into account the conformational relaxation and assuming a conformational temperature of 60 K in the helium expansion.[31] The ratio is in good agreement with the experimental one with the exception of conformer VI, thus reflecting the challenge in calculating relative dissociation energies to sub-kJ mol^{-1} accuracy. Through hydrogen-bonding interactions, *S*-PO successfully locks *gauche* TFE, a transient chiral molecule which is prochiral on average,[1] into a diastereomeric complex and induces a preference between $g+$ and $g-$ TFE. Based on the experimental relative abundance, the overall preference for the $g+$ TFE···*S*-PO versus $g-$ TFE···*S*-PO diastereomers is about 2.8 times at 60 K.

To evaluate the effects of fluorination, we compare the current results with two related model systems, namely ethanol···PO and 2-fluoroethanol···PO. First, fluorination increases the dissociation energies of the most stable group of the binary adducts noticeably from about 16 kJ mol^{-1} for ethanol, to about 18 kJ mol^{-1} for 2-fluroethanol, and finally to about 27 kJ mol^{-1} for TFE, that is, by about 70% over its ethanol counterpart. The effect of ethanol fluorination on the first solvating water molecule was reported recently.[32] For comparison, in the binary adducts of water with ethanol, 2-fluoroethanol, and TFE, where water serves as hydrogen-bond acceptor, the dissociation energies increase from about 19 kJ mol^{-1} to about 26 kJ mol^{-1}, and finally to about 28 kJ mol^{-1}, respectively.[32] It therefore appears that the effect of fluorination on dissociation energy switches on more gradually in the complexes with PO than with water. Second, from the experimental abundances it is evident that ethanol···PO subtly favors *syn* diastereofacial interactions, while both 2-fluroethanol···PO and TFE···PO favor *anti* arrangements. This different preference is not unexpected ecause the F can participate in F···H–C secondary hydrogen bonds with PO, and this arrangement can be better achieved with the oxirane methyl group out of the way, that is, in the *anti* arrangement. The third interesting difference is that while 2-fluoroethanol···PO strongly favors the closed structures with two intermolecular F···H–C bonds, TFE···PO favors the more open structures with just one intermolecular F···H–C bond.

One may initially wonder if E^{int}, the interaction energy of the binary complex, is the cause for such differences in the

mono- and trifluoroethanol adducts. However, a detailed inspection of the various factors which contribute to the stability of the adducts indicates that E^{int} favors the open structures over the closed structures on the order of about 4 kJ mol^{-1}, for both the mono-[19] and trifluoroethanol adducts. Rather, the final differences in preference come from the different monomer stabilities and deformation energies. The penalty to fold TFE into the shape needed for the closed form of TFE··PO versus that for the open form of TFE··PO is about 0.7 kJ mol^{-1}. For 2-fluoroethanol···PO, the open form requires the open *gauche* 2-fluoroethanol subunit, while the closed form requires the compact *gauche* 2-fluoroethanol subunit. Please note that we adopt the *open gauche* and compact *gauche* labels used for the 2-fluoroethanol monomer in reference [17]. The penalty to incorporate the open *gauche* 2-fluoroethanol subunit in the binary adduct versus the compact *gauche* 2-fluroethanol subunit is about 11 kJ mol^{-1}. Consequently, 2-fluoroethanol···PO favors the closed structures over the open ones.

In conclusion, using broadband and narrow-band FTMW spectroscopy in combination with ab initio calculations, we investigated the conformational isomerism of an important chirality induction model system, that is, TFE···PO, in great detail. The identities of the four observed conformers were unequivocally established. Furthermore, from the broadband measurements, we were able to deduce reliable conformational abundances and propose possible conformational conversion paths which reduce the observable conformers from eight to four in a jet expansion. A strong preference for the *g* + TFE···*S*-PO diastereomers versus *g*− TFE···*S*-PO was observed, although to a much lesser degree compared to the TFE dimer case where only one homochiral species was detected experimentally.[14] We further show that fluorination has great effects on the overall binding strength of the binary adducts and on the corresponding conformational distribution.

Received: March 30, 2014
Revised: May 7, 2014
Published online: June 4, 2014

Keywords: chirality · computational chemistry · conformation analysis · perfluorinated solvents · rotational spectroscopy

[1] A. Zehnacker, M. A. Suhm, *Angew. Chem. Int. Ed.* **2008**, *47*, 6970 – 6992; *Angew. Chem.* **2008**, *120*, 7076 – 7100.
[2] J. Halpern, *Science* **1982**, *217*, 401 – 407.
[3] R. A. Sheldon, *Chirotechnology: Industrial Synthesis of Optically Active Compounds*, Marcel Dekker, New York, **1993**, pp. 39 – 72.
[4] R. E. Morris, X. Bu, *Nat. Chem.* **2010**, *2*, 353 – 361.
[5] A. R. A. Palmans, E. W. Meijer, *Angew. Chem. Int. Ed.* **2007**, *46*, 8948 – 8968; *Angew. Chem.* **2007**, *119*, 9106 – 9126.
[6] G. Celebre, G. De Luca, M. Maiorino, F. Iemma, A. Ferrarini, S. Pieraccini, G. P. Spada, *J. Am. Chem. Soc.* **2005**, *127*, 11736 – 11744.
[7] a) K. Shiraki, K. Nishikawa, Y. Goto, *J. Mol. Biol.* **1995**, *245*, 180 – 194; b) K. Gast, D. Zirwer, M. M. Frohone, G. Damaschun, *Protein Sci.* **1999**, *8*, 625 – 634; c) P. Luo, R. L. Baldwin, *Biochemistry* **1997**, *36*, 8413 – 8421.
[8] V. A. Soloshonok, *Angew. Chem. Int. Ed.* **2006**, *45*, 766 – 769; *Angew. Chem.* **2006**, *118*, 780 – 783.
[9] J. F. Povey, C. M. Smales, S. J. Hassard, M. J. Howard, *J. Struct. Biol.* **2007**, *157*, 329 – 338.
[10] a) M. Buck, *Q. Rev. Biophys.* **1998**, *31*, 297 – 355; b) M. Fioroni, M. D. Diaz, K. Burger, S. Berger, *J. Am. Chem. Soc.* **2002**, *124*, 7737 – 7744.
[11] R. Carrotta, M. Manno, F. M. Giordano, A. Longo, G. Portale, V. Martorana, P. L. San Biagio, *Phys. Chem. Chem. Phys.* **2009**, *11*, 4007 – 4018.
[12] H. C. Hoffmann, S. Paasch, P. Müller, I. Senkovska, M. Padmanaban, F. Glorius, S. Kaskel, E. Brunner, *Chem. Commun.* **2012**, *48*, 10484 – 10486.
[13] D. Hamada, F. Chiti, J. I. Guijarro, M. Kataoka, N. Taddei, C. M. Dobson, *Nat. Struct. Biol.* **2000**, *7*, 58 – 61.
[14] a) T. Scharge, T. Häber, M. A. Suhm, *Phys. Chem. Chem. Phys.* **2006**, *8*, 4664 – 4667; b) T. Scharge, C. Cézard, P. Zielke, A. Schütz, C. Emmeluth, M. A. Suhm, *Phys. Chem. Chem. Phys.* **2007**, *9*, 4472 – 4490; c) T. Scharge, T. N. Wassermann, M. A. Suhm, *Z. Phys. Chem.* **2008**, *222*, 1407 – 1452.
[15] C. Pérez, M. T. Muckle, D. P. Zaleski, N. A. Seifert, B. Temelso, G. C. Shields, Z. Kisiel, B. H. Pate, *Science* **2012**, *336*, 897 – 901.
[16] I. Peña, E. J. Cocinero, C. Cabezas, A. Lesarri, S. Mata, P. Écija, A. M. Daly, Á. Cimas, C. Bermúdez, F. J. Basterretxea, S. Blanco, J. A. Fernández, J. C. López, F. Castaño, J. L. Alonso, *Angew. Chem. Int. Ed.* **2013**, *52*, 11840 – 11845; *Angew. Chem.* **2013**, *125*, 12056 – 12061.
[17] J. Thomas, F. X. Sunahori, N. Borho, Y. Xu, *Chem. Eur. J.* **2011**, *17*, 4582 – 4587.
[18] N. Borho, Y. Xu, *Angew. Chem. Int. Ed.* **2007**, *46*, 2276 – 2279; *Angew. Chem.* **2007**, *119*, 2326 – 2329.
[19] N. Borho, Y. Xu, *J. Am. Chem. Soc.* **2008**, *130*, 5916 – 5921.
[20] a) G. G. Brown, B. C. Dian, K. O. Douglass, S. M. Geyer, B. H. Pate, *J. Mol. Spectrosc.* **2006**, *238*, 200 – 212; b) G. S. Grubbs II, C. T. Dewberry, K. C. Etchison, K. E. Kerr, S. A. Cooke, *Rev. Sci. Instrum.* **2007**, *78*, 096106.
[21] L. H. Xu, G. T. Fraser, F. J. Lovas, R. D. Suenram, C. W. Gillies, H. E. Warner, J. Z. Gillies, *J. Chem. Phys.* **1995**, *103*, 9541 – 9548.
[22] T. Goldstein, M. S. Snow, B. J. Howard, *J. Mol. Spectrosc.* **2006**, *236*, 1 – 10.
[23] Gaussian 09 (Revision C.01): M. J. Frisch, et al. See the Supporting Information for the full reference.
[24] I. Bako, T. Radnai, M. Claire, B. Funel, *J. Chem. Phys.* **2004**, *121*, 12472 – 12480.
[25] a) S. Dempster, O. Sukhrukov, Q. Y. Lei, W. Jäger, *J. Chem. Phys.* **2012**, *137*, 174303; b) J. Thomas, J. Yiu, J. Rebling, W. Jäger, Y. Xu, *J. Phys. Chem. A* **2013**, *117*, 13249 – 13254.
[26] a) T. J. Balle, W. H. Flygare, *Rev. Sci. Instrum.* **1981**, *52*, 33 – 45; b) J.-U. Grabow, W. Stahl, H. Dreizler, *Rev. Sci. Instrum.* **1996**, *67*, 4072 – 4084.
[27] Y. Xu, W. Jäger, *J. Chem. Phys.* **1997**, *106*, 7968 – 7980.
[28] "Aspects of Quartic and Sextic Centrifugal Effects on Rotational Energy Levels": J. K. G. Watson in *Vibrational Spectra and Structure*, *Vol. 6* (Ed.: J. R. Durig), Elsevier, Amsterdam, **1977**, p. 39.
[29] PGOPHER, a Program for Simulating Rotational Structure, C. M. Western, University of Bristol, http://Pgopher.chm.bris.ac.uk.
[30] a) S. S. Xantheas, *J. Chem. Phys.* **1996**, *104*, 8821 – 8824; b) K. Szalewicz, B. Jeziorski, *J. Chem. Phys.* **1998**, *109*, 1198 – 1200.
[31] N. Borho, Y. Xu, *Phys. Chem. Chem. Phys.* **2007**, *9*, 4514 – 4520.
[32] M. Heger, T. Scharge, M. A. Suhm, *Phys. Chem. Chem. Phys.* **2013**, *15*, 16065 – 16073.

